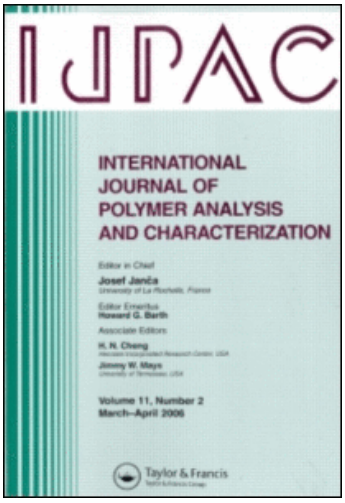

International Journal of Polymer Analysis and Characterization
Publication details, including instructions for authors and subscription information:
http://www.informaworld.com/smpp/title~content=t713646643

Luminescence Studies of Pr^{3+} Doped Chitosan Biocomposite Matrix through UV Radiation Induced Thermal Stimulation

Ravish Kumar[a]
[a] Department of Mechanical Engineering, Maulana Azad National Institute of Technology, Bhopal, India

Online publication date: 04 June 2010

To cite this Article Kumar, Ravish(2008) 'Luminescence Studies of Pr^{3+} Doped Chitosan Biocomposite Matrix through UV Radiation Induced Thermal Stimulation', International Journal of Polymer Analysis and Characterization, 13: 4, 254 — 268
To link to this Article: DOI: 10.1080/10236660802141008
URL: http://dx.doi.org/10.1080/10236660802141008

International Journal of Polymer Anal. Charact., 13: 254–268, 2008

ISSN: 1023-666X print
DOI: 10.1080/10236660802141008

Taylor & Francis
Taylor & Francis Group

Luminescence Studies of Pr^{3+} Doped Chitosan Biocomposite Matrix through UV Radiation Induced Thermal Stimulation

Ravish Kumar
Department of Mechanical Engineering, Maulana Azad National Institute of Technology, Bhopal, India

Abstract: Thermoluminescence of Pr^{3+} doped chitosan biocomposite matrix (CBM) has been investigated. The polycrystalline sample of the matrix was prepared by the conventional solid-state reaction method. The formation of calcium sulfide in this process is checked for crystallization and phase by X-ray diffraction study, and the sample is found to have a rock salt structure at room temperature. Thermally stimulated luminescence studies of the matrix sample irradiated by a UV source show one prominent glow peak around 492.7 K and a shoulder peak around 370 K when heated with a linear heating rate of 2°C/s. The two glow peaks were isolated via thermal cleaning and a detailed kinetic analysis has been performed by various methods of determining the trap parameters, namely, order of kinetics (*b*), activation energy (*E*), and frequency factor (*s*) associated with both peaks of the CBM:Pr^{3+} matrix. A critical survey of the methods of determining E in our sample is undertaken to extend the domain of application as far as possible. We comment on the comparison between the derived parameter values and the correct values. From these comparisons we attempt to obtain some useful insights to assist in the interpretation of experimentally observed thermoluminescence spectra.

Keywords: Calcium sulfide matrices; Solid-state reaction; Thermal cleaning; Thermoluminescence; X-ray diffraction

Received 8 February 2008; accepted 10 April 2008.
Correspondence: Ravish Kumar, Department of Mechanical Engineering, Maulana Azad National Institute of Technology, Bhopal (MP) 462003, India. E-mail: ravishk@rediffmail.com

INTRODUCTION

Polyelectrolytes form the second largest class of stimulus-responsive polymers used in affinity precipitation. Chitosan is one of these. Chitosan biocomposite matrices (CBM) have been widely reported in the literature as an excellent matrix for a quite long time now. The luminescent properties of CBM with a rare earth ion activator have drawn considerable attention due to their potential use for cathode ray tubes, infrared sensors, thermoluminescent dosimeter, electroluminescence panels, and near-infrared to visible converters and magneto-optical devices.[1,2] Polymers like chitosan and some cellulose derivatives carry both ionogenic and hydrophobic groups within the molecule. The ionogenic groups may be protonated or not depending on the pH. If these groups are uncharged, the hydrophobic character of the polymer dominates and the water solubility is low. If the ionogenic groups are charged, the polyelectrolytic character becomes predominant and the polymer is highly soluble in water. The solubility of such molecules is therefore a function of the pH.

Modified chitosans have been prepared with various chemical and biological properties. *N*-Carboxymethylchitosan and *N*-carboxybutylchitosan have been prepared for use in cosmetics and in wound treatment. Several polysaccharide-based biopolymers are being used as possible coating materials or packaging films. They include starch, pullulan, and chitosan. The degradation of synthetic polymer films can be accelerated by incorporating starch as a filler. Low-density polyethylene (LDPE) blends with up to 10% cornstarch were produced using conventional techniques and were made into bags for groceries or rubbish. Although CBM is one of the oldest luminescent materials, there is a comparative lack of information about the defect properties in these materials, especially those doped with Pr^{3+}, to the best of our knowledge. It is well known that trapping centers play an essential role for photo energy storage in persistent, photo-stimulable, and thermo-stimulable matrixes. In order to elucidate information about luminescence process of matrices, knowledge of defect structures and the distribution of energy levels in the band gap of solids is very essential. Usually, information about the trapping levels can be obtained by thermoluminescence (TL) measurements in which irradiation transfers electrons to the traps. After turning off the irradiation source, the thermally stimulated luminescence is monitored under a condition of uniformly increasing temperature. The shape and position of the resultant TL glow curves can be analyzed to extract information on the various parameters of the trapping process—trap depth, escape frequency, trapping and retrapping rates, etc.

A series of peaks appearing on the TL curve may be attributed to trap levels characterized by different activation energies. Detailed studies

of the TL spectra of rare earth element (REE) dopants in insulators show that the maxima in the luminescence intensity during heating of irradiated material (i.e., the glow peak temperatures) differ as a result of the ion size and that the emission is typical for trivalent REE, which would be the appropriate emission sites on many of the TL models.[3,4] Compared with the study of emission centers, trapping dynamics is more complicated and the nature of trapping centers has been studied to a lesser extent. It should be noted that knowledge of the kinetic parameters is important in understanding TL phenomena as well as in the practical use of the thermoluminescent material as dosimeters. Thus, the aim of the present work is to undertake a detailed kinetic analysis of the CBM matrix system and to evaluate the kinetic parameters, namely, activation energy E, frequency factor s, and kinetic order b, via various methods widely reported in the literature. To completely characterize the luminescence properties of these materials, the obtained TL glow curves were analyzed to determine the evolution of the kinetic parameters with irradiation. Analysis of the glow curves to ascertain the kinetic parameters describing each component is explained in this article. Usually, the glow curves are analyzed in terms of either first-order (where the intensity of the TL is proportional to the concentration of thermally released charges) or second-order kinetics (the thermally released charges are retrapped at least once before the recombination process). However, here we use a computerized curve fitting based on general-order kinetics to be used for the characterization of the most useful parameters.

KINETIC ANALYSIS AND KINETIC EQUATIONS

Computerized glow curve deconvolution used in thermoluminescence (TL) dosimetry and based on fitting methods depends on the shape assumed for single glow peaks, i.e., on the mathematical equations provided by TL models.[5,6] The use of some synthetic dosimeters as well as some natural materials giving glow curves that cannot be well fitted by first-order or second-order kinetics made necessary the use of new peak shape functions based on more complex descriptions of TL processes. Unfortunately, most of these descriptions do not yield explicit expressions suitable for fitting algorithms. Although there is not an agreement about what model should be preferred, the generally good fits of many experimental glow curves by the so-called general- and mixed-order kinetics makes them good candidates to be considered as simplified descriptions of TL mechanisms for glow curve analysis in TL dosimetry.

May and Partridge[7] and others have proposed an empirical equation to describe the TL glow peak when conditions for neither first- nor second-order kinetics are satisfied. This equation is known as the

general-order (GO) kinetics and its final form is given by Equation (1). The mathematical expression of GO kinetics and related discussions about it may be found in many places in the literature.[8,9]

When a linear heating profile, $T(t) = T_0 + \beta t$, is applied, the general-order expression for each glow peak can be written in terms of the kinetic parameters (E, s, and b) as:

$$I(T) = sn_0 \exp\frac{E}{kT}\left\{1 + (b-1)\frac{s}{\beta}\int_{T_0}^{T}\exp\left(\frac{-E}{kT}\right)\right\} \tag{1}$$

where n_0 is the initial density of trapped charge carriers, s is the frequency factor, and k is the Boltzmann constant.

Or using the maximum condition set as $\frac{dI(t)}{dt} = 0$:

$$I(T) = I_M \exp\left(\frac{E}{kT_M}\right)\left\{1 + \left(1 - \frac{1}{b}\right)\frac{E}{kT_M^z}\int_{T_M}^{T}\exp\left(\frac{E}{kT_M} - \frac{E}{kT'}\right)dT'\right\} \tag{2}$$

where T_M and I_M are the temperature and the intensity of the maximum. The integral in Equations (1) and (2) cannot be solved in terms of elementary functions. One of the simplest possible approximations to evaluate Equation (2) is to consider:

$$\exp\left(\frac{E}{kT_M} - \frac{E}{kT}\right) \approx \exp\left[\frac{E}{kT_M^z}(T - T_M)\right] \tag{3}$$

and

$$\frac{E}{kT_M^2}\int_{T_M}^{T}\exp\left(\frac{E}{kT_M} - \frac{E}{kT'}\right)dT' \approx \exp\left[\frac{E}{kT_M^2}(T - T_M)\right] - 1 \tag{4}$$

Thus the general-order fitting function can be written as

$$I(T) = I_M \exp\left[\frac{E}{kT_M^2}(T - T_M)\right]\left\{\frac{1}{b} + \left(\frac{b-1}{b}\right)\exp\left[\frac{E}{kT_M^2}(T - T_M)\right]\right\} \tag{5}$$

DETERMINATION OF TRAP PARAMETERS

We adopted a systematic approach as suggested by Chen et al.[10] to analyze the TL glow curve. A rough estimate of E was carried over using the conventional initial rise (IR) method. According to Garlick and Gibson,[11] at the beginning of the TL glow, just before the inflection point on the rising part of the peak, the variation of the integral compared in the kinetics equation can be neglected, so that

Equation (1) simply becomes

$$I = C\exp\left(\frac{-E}{kT}\right)$$

which is independent of the kinetics order. A plot of ln (I) against $1/kT$ should be a straight line in the initial rise region. The slope of this straight line allows readily finding the value of E. To avoid error due to a decrease in the number of electrons remaining trapped, it is necessary to restrict the temperature range corresponding to 11 experimental data points. However, the intensity at the beginning of each peak is very low, so the inaccuracies could be high. Furthermore, a spread in trap depths can lead to the glow continuing to increase instead of reaching the point of inflection. To overcome the constraint of using a limited number of experimental data in the IR method, we preferred to apply the whole glow peak area method in which the area n (T) under the glow peak is calculated starting at temperature T to the maximum temperature available. Graphs of ln (intensity/area^b) versus $1/kT$ are drawn for several values of kinetic order b. The value of b that gives the best-fit straight line was chosen as final. Also, E can be estimated from the slope of this straight line.

Kinetic orders (b) of the two separated peaks were determined using Shenker and Chen's geometry factors[8]: $\mu_g = \delta/\omega$, where $\omega = T_2 - T_1$ is the total half-width and $\delta = T_2 - T_m$ is the half-width at the high temperature side of the peak. The equation

$$E_\alpha = C_\alpha\left(\frac{kT_M^2}{\alpha}\right) - b_\alpha(2kT_M) \tag{6}$$

is used for calculation of the activation energy E, where $\alpha = \tau$, δ, or ω and

$$C_\tau = 1.51 + 3.0\ (\mu_g - 0.42); \quad b_\tau = 1.58 + 4.2(\mu_g - 0.42) \tag{7}$$

$$C_\delta = 0.976 + 7.3\ (\mu_g - 0.42); \quad b_\delta = 0 \tag{8}$$

$$C_\omega = 2.52 + 10.2\ (\mu_g - 0.42); \quad b_\omega = 1 \tag{9}$$

and $\tau = T_m - T_1$, which is the half-width at low temperature of the peak. The frequency factors s were calculated using the following equation:

$$\frac{\beta}{T_M^2} = \left(\frac{sk}{E}\right)[1 + (b-1)\Delta_M]\exp\left(\frac{2E}{kT_M}\right) \tag{10}$$

where β is the heating rate, T_m is the maximum temperature of the peak, $\Delta_m = 2kT_m/E$, and k is the Boltzmann constant. The values obtained for E_α, s_α ($\alpha = \tau$, δ, ω), and b are given in Table I.

Table I. Kinetic analysis using whole glow peak method

Glow curve	Kinetic order b	Activation energy E (eV)	Intercept	Pre-exponential frequency factor s ($\sec^{-1}$) $s' = \beta\, e^{(\text{intercept})}$	Regression coefficient R
First	2.4	0.687 ± 0.003	10.97 ± 0.129	$\pm\ (1.162 \pm 0.14) \times 10^5$	0.999
Second	0.9	0.587 ± 0.054	10.79 ± 0.130	$\pm\ (1.162 \pm 0.15) \times 10^5$	0.998

EXPERIMENTATION

The doped chitosan biocomposite matrix was prepared via the conventional solid-state reaction method. Chitosan biocomposite matrix, $CBMO_4{\cdot}2H_2O$, sodium thiosulfate (flux) (British Drug House), and praseodymium oxide, Pr_2O_3 (99.99%, S.D. Fine Chemicals India) were used as starting materials. The rare earth oxide was dissolved in concentrated nitric acid and was added in a concentration of 0.01% by weight. The starting compositions were well mixed in stoichiometric ratios using a slurry mixing technique. The charge after drying overnight in an oven was placed in a graphite crucible, and some active carbon powder layer was sprayed onto it. The crucible was covered with another graphite crucible containing active carbon powder to make a semi-airtight chamber at elevated temperatures and to avoid the oxidation of the products in the heating stage. Thus, the charge was fired in a reductive atmosphere of carbon in a muffle furnace at 1000°C for 2 h. The charge was rapidly pulverized while red hot for effective trapping of activator atoms. The final phases of the product were checked with a conventional X-ray diffraction (XRD) technique at room temperature in a wide range of Bragg angles ($10^\circ \leq 2\theta \leq 80^\circ$) using a Holland PW 1710 X-ray diffractometer with Cu target and at a scanning rate of 3°/min. The X-ray diffraction pattern for the matrix prepared as above showed that it was crystallized in a rock salt–type structure and that there was no detectable trace of sulfates or oxides. The thermostimulation luminescence (TSL) studies were made by using an integral PC–based thermoluminescence reader system (TL 10091) supplied by Nucleonix Systems (India). The samples were irradiated by an Ultra Vitalux (Germany) 300 W UV lamp. The glow curves were recorded by heating the sample at a linear heating rate of 2°C/s, and the luminescence emission was detected by a photomultiplier tube (type 9924) imported from the U.K. The time duration between the irradiation and TL readout was always kept constant at about 5 min. The samples were annealed at 300°C at a linear heating rate of 2°C/s prior to subsequent irradiation during each experiment to erase

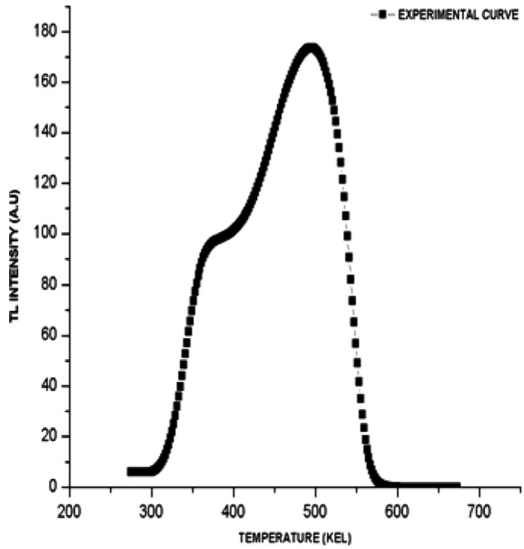

Figure 1. Thermoluminescence glow curve of CBM:Pr^{3+}.

any residual information and then cooled in air to room temperature. During the experiments, the sample was read twice. The second reading with the same temperature profile is considered to be the background of the readout plus sample and was subtracted digitally from the first one.

The typical experimental glow curve obtained for the sample containing activator Pr^{3+} (0.01%) is shown in Figure 1. The time scale has been changed to a corresponding temperature scale by multiplying it with the constant heating rate. The glow curve shows one prominent thermoluminescence (TL) peak at around 492.7 K (II peak) and a shoulder peak at around 370 K (I Peak). The two overlapping peaks were separated via a thermal cleaning method following a two-stage readout process. The first stage (the preheat phase) is designed to evolve the low-temperature peak without depopulating the electron-trapping center responsible for higher peak. The temperature is then rapidly increased and maintained until the TL signal from the higher trap is evolved.

RESULTS AND DISCUSSIONS

Figure 2 shows the XRD patterns of the CBM: Pr^{3+} matrix. All the peaks can be indexed to the cubic phase of CBM of the Joint Committee

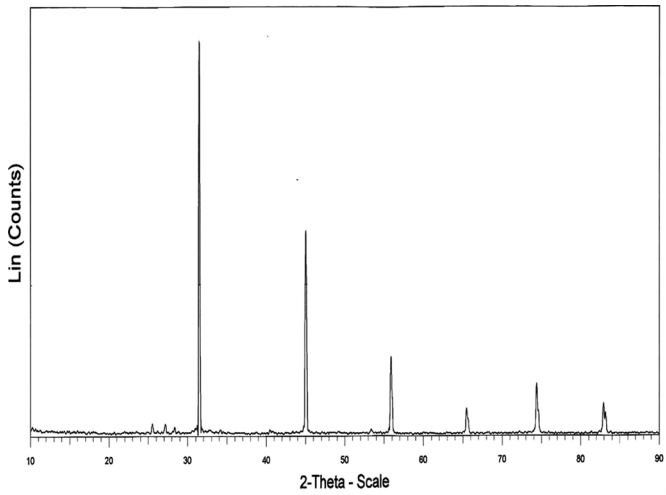

Figure 2. X-ray diffraction spectra of CBM: Pr^{3+} (0.01% by weight).

on Powder Diffraction Data Standards (JCPDS) Diffraction Data File No. 25–134, indicating that the doping ions did not form any new phases in the synthesis process.

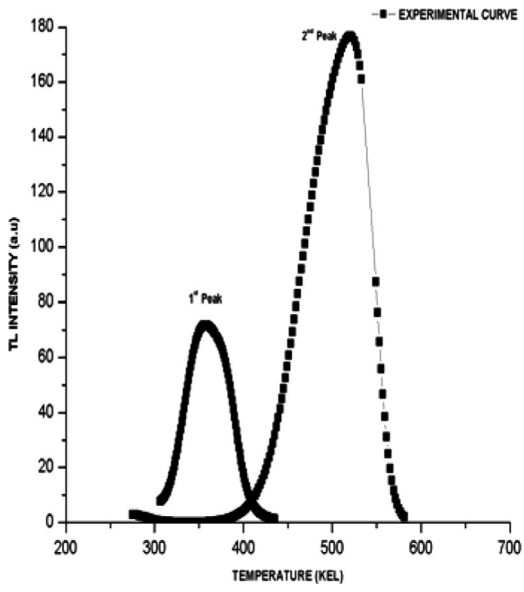

Figure 3. Separated peaks (first and second) shown as a result of thermal cleaning process.

As stated earlier, thermal cleaning was applied to isolate the peaks of interest. These isolated glow curves are shown in Figure 3. It is noteworthy that peak shifts corresponding to both peaks (first peak T_m shifts from 370 to 356.64 K and second peak T_m shifts from 492.7 to 521 K) are observed as a result of thermal cleaning. The values of E may be considerably affected owing to this shift. We started the analysis using the classical IR method that is independent of shape of the peak. Several portions of the initial part of the peaks were received and analyzed. The data range for the IR plot of the second peak, shown in Figure 5, was chosen after the first peak maximum. Thus, the experimental data range corresponding to the central portion on the rising edge of the second peak was chosen to estimate the E values. A semilog plot of I versus $1/kT$, acting as a linearizing transformation, gives an E evaluation that doesn't depend on s. Figures 4 and 5 show the IR plot and the best-fit straight lines for the two isolated peaks, the slopes of which give an estimation of E. A noticeable deviation from a straight line for the second glow curve IR plot, as shown in Figure 5, may be due to the presence of traps with slightly different activation energies than that reported in our result. This component of E could be due to the contribution of another peak(s) at high temperature just at the start of the second peak, which cannot be further resolved from the main second peak, or to an unknown mechanism that is operative when the sample is held to a stable high temperature. This possibility inspired us to take a view of the glow curve structure

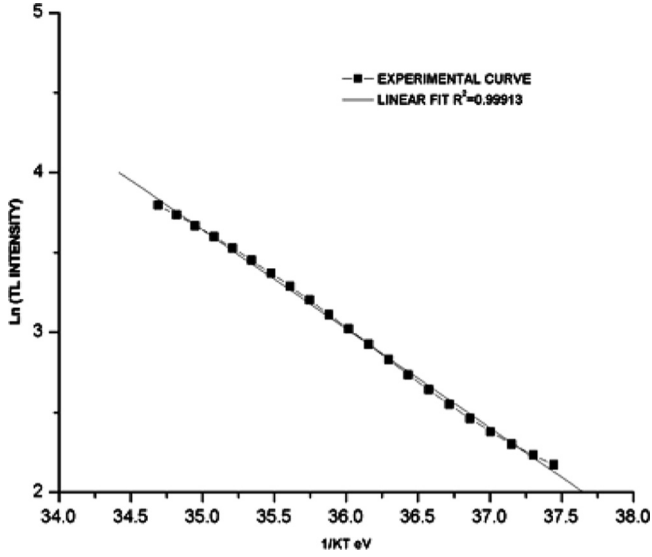

Figure 4. Applying IR method to first peak.

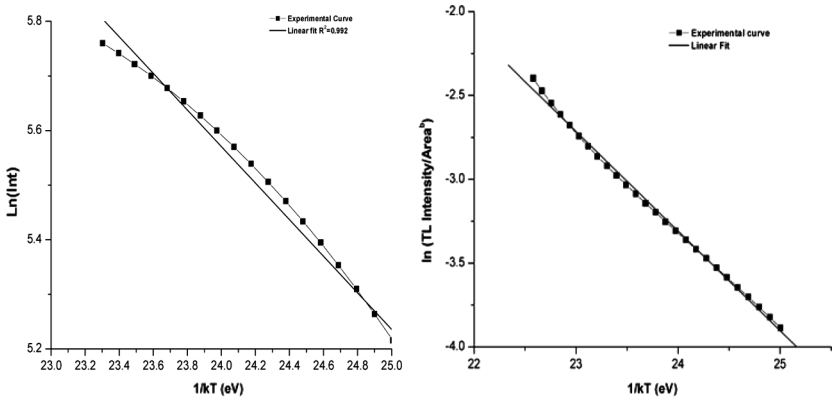

Figure 5. Applying IR method to second peak.

just at the overlap of the prominent and shoulder peak. The glow curve structure corresponding to the shoulder peak was obtained by digitally subtracting the isolated second glow curve from the combined experimental glow curve. This is shown in Figure 9. The somewhat flattened shape of the first peak around the maximum suggests the possibility of clustered trap groups having trap depth close to each other. The resulting values of the activation energy are (0.619 ± 0.005) and (0.317 ± 0.009) for the first and second peak respectively.

The consistencies of E values obtained by the IR method were further checked by another peak shape–independent method. This is well known in the literature as the whole glow peak area method[7] and depends on the surface subtended by the glow curve between two given temperatures, i.e., area. The area under the glow peak was calculated using graphical integration, and a graph of Ln (TL intensity/area^b) was plotted. Setting different values of kinetic order b, we carried out statistical optimization using the linear fit tool of the Origin 6.1 software package until a best-fit straight line was obtained. Kinetic order values $b = 2.4$ and $b = 0.9$ resulted in best-fit straight lines with the highest coefficient of regression R for the first and second peak as 0.999 and 0.998 respectively. The plots are shown in Figures 5 and 6.

The whole glow peak method yields information about both the activation energy E and the effective frequency factors s' and $s'' = s' n_0^{(b-1)}$ appearing in Equation (1). The value of n_0 can be estimated from the area of the glow curves. The results obtained with this method are given in Table I. The E value obtained by this method for the first glow curve can be considered to be in good agreement with that obtained by the IR method. For the second glow curve, the IR method predicts quite a

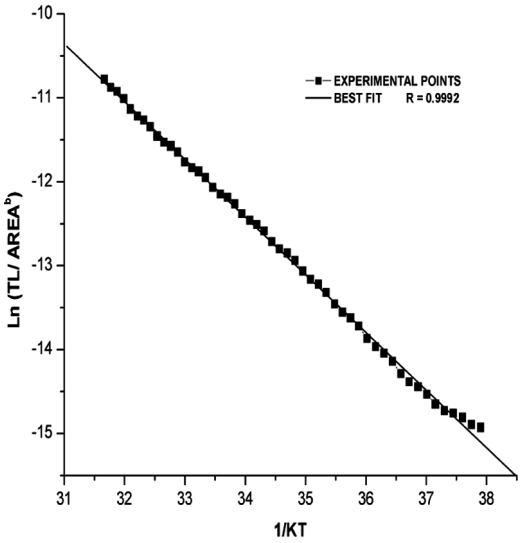

Figure 6. Applying whole peak method on second peak.

low value of E due to the reasons previously mentioned. Shenker and Chen's peak shape method was found to be a suitable choice among the various peak shape–dependent methods reported in the literature. By determining the maximum and the half-intensity temperatures, geometrical factors (μ_g) were calculated for the two isolated glow curves. The μ_g values did not correspond to that reported for either first- or second-order kinetics. We have verified the order of kinetics corresponding to our μ_g values from the calculated graph of μ_g ranging from 0.36 to 0.55 for values of b between 0.7 and 2.5 reported by Chen et al.,[2] and the results seem to be in good agreement. Once the activation energy is obtained, the frequency factor was calculated from Equation (10) by using E_τ value. Table II shows the result of the use of Shenker and Chen's method.

Table II. Kinetic analysis using Shenker and Chen's peak shape method

Peak	Geometrical factor (μ_g)	Activation energy E (eV)			Frequency factor s (s^{-1})
		E_τ	E_δ	E_ω	
First	0.56	0.54	0.31	0.39	0.42×10^4
Second	0.33	0.60	1.34	0.88	0.36×10^7

Finally, glow curve fitting was applied using the fitting function for general-order kinetics given by Equation (5). The expression relies on two experimentally measured quantities, I_M (the maximum TL intensity) and T_M (the temperature corresponding to the maximum TL intensity). By treating E as an adjustable parameter, we calculated several graphs. A best fit, indicated by the lowest figure of merit ($\text{FOM} = \Sigma \mid \text{TL}_{\text{experimental}} - \text{TL}_{\text{fit}})/\Sigma\, \text{TL}_{\text{fit}}$), was obtained for E values 0.687 and 0.594 eV for the first and second glow curve respectively as shown in Figures 7 and 8. Finally, the fitted E values were used in Equation (10) to calculate the frequency factor.

$$\text{First curve}: s = 7.2 \times 10^8\ \text{s}^{-1}$$

$$\text{Second curve}: s = 0.7 \times 10^4\ \text{s}^{-1}$$

As can be seen from Figures 7 and 8, the theoretically generated glow curve fits reasonably well with rising portions of the experimental curves on the lower temperature side. The FOM values obtained for the first and second glow curve are 14.56% and 16.03% respectively. It was not possible to obtain the ideal value of FOM ($\leq$5%) as reported for any other fitting parameter other than that used. The marginal fitting on the higher temperature side in both isolated glow curves may be due to the presence of some more peaks that were not resolved using the thermal cleaning

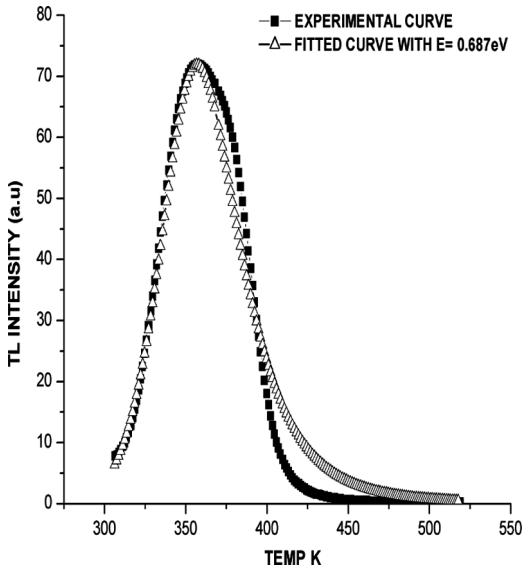

Figure 7. First glow curve: experimental data.

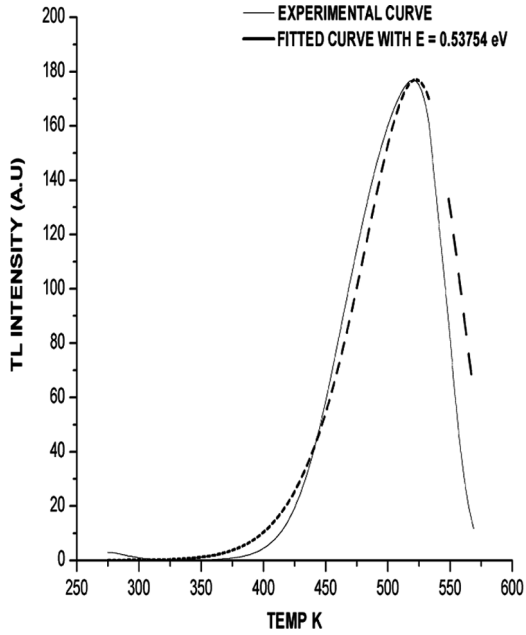

Figure 8. Second glow curve: Experimental data and numerically fitted TL.

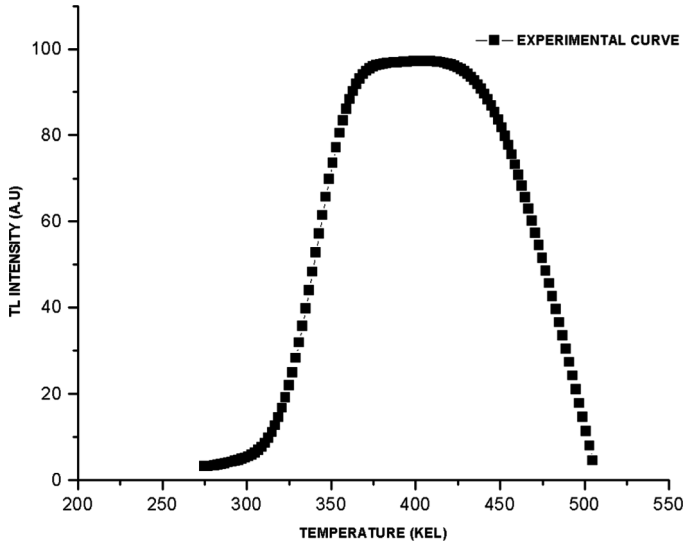

Figure 9. First peak glow curve structure obtained by subtracting the second isolated glow curve from the combined experimental curve.

procedure. Further work is in progress to obtain better results using computerized glow curve deconvolution functions (CGCD) that may reveal other overlapping peaks without the use of thermal cleaning. In order to obtain more information about the processes involved, the kinetic analysis should also be carried out for glow peaks measured under different heating rates, various irradiation doses, etc. We also realize the importance of other studies, like thermally stimulated conductivity (TSC) and electron spin resonance (ESR), that should be undertaken together with TL to get a deeper insight of trap dynamics.

CONCLUSIONS

CBM: Pr^{3+} matrix is synthesized via the solid-state diffusion method, and attempts to determine the kinetic parameters by applying several methods are presented. However, the main problem measuring the trap parameters is the presence of several overlapping peaks within the TL glow curve. Although thermal cleaning proves to be successful in isolating the prominent and shoulder peaks of the sample, the presence of some more overlapping peaks, having activation energies close to one another, just at the co-juncture of the first and second glow curve cannot be exactly ruled out. The residual plots obtained after subtracting the second isolated glow curve from the combined experimental glow curve reveals this fact very well (see the somewhat flattened peak shape in Figure 9).

The study begins with obtaining the trap parameters of the isolated glow peaks. Using both peak shape–dependent and peak shape–independent methods, we have been able to get an approximation of activation energy E and kinetic order b. An important consideration was made while applying the IR method in deciding the region of the individual glow curves to be used for regression analysis of the graph Ln (intensity) versus $\frac{1}{kT}$, especially for the second glow curve The kinetic order obtained via the whole glow peak method suggests the possibility of a general-order TL process. This led us to finally use a numerical curve-fitting technique using a general-order fitting function to obtain the results.

REFERENCES

[1] Zhan, Li., and Yumin, Du. (2003). Preparation and characterization of CdS quantum dots chitosan biocomposite. *React Funct. Polym.* **55**(1), 35–43.

[2] Chen, W. C. W., D. J. Maxwell, X. Gao, R. E. Bailey, M. Han, and S. Nie. (2002). Luminescent quantum dots for multiplexed biological detection and imaging. *Curr. Opin. Biotechnol.* **13**, 40–46.

[3] Oczkowski, H. L. (1982). Thermoluminescence model with intra-pair metastable state. *Phys. Status Solidi A* **74**(1), 65–74.
[4] Oczkowski, H. L. (1984). The retrapping process in a thermoluminescence model with an intra-pair metastable state. *Phys. Status Solidi A* **82**(1), 213–219.
[5] Pagonis, V., G. Kitis, and R. Chen. (2003). Applicability of the Zimmerman predose model in the thermoluminescence of predosed and annealed synthetic quartz samples. *Radiat. Meas.* **37**(3), 267–274.
[6] van Dijk, J. W. E. (2006). Thermoluminescence glow curve deconvolution and its statistical analysis using the flexibility of spreadsheet programs. *Radiat. Protect. Dosimetry* **119**(1–4), 332–338.
[7] May, C. E., and J. A. Partridge. (1965). Anomalous thermoluminescent kinetics of irradiated alkali halides. *J. Chem. Phys.* **42**, 797–798.
[8] Shenker, D., and R. Chen. (1971). Numerical curve fitting of general order kinetics glow peaks. *J. Phys. D Appl. Phys.* **4**, 287–291.
[9] Sunta, C. M., W. E. Feria Ayta, R. N. Kulkarni, R. Chen, and S. Watanabe. (1997). Pre-exponential factor in general order kinetics of thermoluminescence and its influence on glow curves. *Radiat. Protect. Dosimetry* **71**, 93–97.
[10] Chen, R., S. W. S. McKeever, and S. A. Durrani. (1981). Solution of the kinetics equations governing trap filling: Consequences concerning the dose dependence and dose-rate effects. *Phys. Rev. B.* **24**, 4931–4944.
[11] Garlick, G. F. J., and A. F. Gibson. (1949). Dielectric changes in phosphors containing more than one activator. *Proc. Phys. Soc. A* **62**, 731–736.